JOURNAL OF MATERIALS SCIENCE 22 (1987) 63–75

Characteristics of high temperature cementitious lost-circulation control materials for geothermal wells

T. SUGAMA, L. E. KUKACKA, B. G. GALEN, N. B. MILESTONE
Process Sciences Division, Department of Applied Science, Brookhaven National Laboratory, Upton, New York 11973, USA

Materials systems have been formulated for the *in situ* conversion of water-based bentonite drilling fluids into cementitious lost-circulation control materials (CLCM) for use in geothermal wells at temperatures up to 300° C. The formulations consist of a cement hardener, a borax admixture, and a fibre glass bridging material which are added to the bentonite fluids. Evaluations of the properties of the slurry and the cured CLCMs revealed that the ions supplied by dissociation of the borax in the CLCM slurry acted to suppress the bentonite hydration and retarded the hardening rate of the cement at elevated temperatures. The CaO–SiO_2–H_2O (C–S–H) phases formed during curing of the CLCM play essential roles in improving the quality of the hardened CLCMs. It was observed that xonotlite—truscottite transformations resulted in strength reductions and increased water permeability. The plugging ability of fibre glass depends on the concentration and fibre size. The silicate ions dissolved by hot alkaline disintegration of the fibreglass were chemisorbed with Ca^{2+} ions from the cement and led to the precipitation of C–S–H compounds on the fibre surfaces, which improved bond strength at the matrix–fibre interfaces.

1. Introduction

Ideally, it should be possible to solve lost-circulation problems in geothermal wells by the direct addition to water-based drilling fluids of a material that forms a slurry, which is pumpable under hydrothermal conditions up to 300° C, and thus can be circulated to a formulation in which loss of fluid occurs. In addition, the material should be capable of converting the drilling mud into a hardened mass which has adequate strength within approximately two hours after plugging the cavernous and highly fractured zones. It has been estimated that the solidified material must have the following minimum characteristics at 300° C to act as an effective seal in a cementitious lost-circulation control material (CLCM) [1]: (i) compressive strength > 3.45 MPa at an autoclaving age of 2 h, (ii) permeability to water $< 1 \times 10^{-2}$ Darcys, and (iii) an increase in volume upon curing.

In oil wells in which the bottom hole temperature never exceeds 150° C, conventional Portland cements are frequently used for lost-circulation control materials [2]. This is convenient since cement is readily available at all well sites. Unfortunately, the common cement plugging systems, which consist of perlite, cement, and silica flour, often give unsatisfactory results, particularly on the first attempt, primarily because the downhole temperature is not known accurately enough to determine the needed amount of retarder [3].

Diesel oil–bentonite–cement gunk squeezes [4–6] are used successfully by the petroleum industry to control total lost circulation, but not generally in geothermal drilling because of environmental objections to the diesel oil component [7].

The use of the sodium silicate, which is environmentally acceptable, is very attractive since cementing equipment and cement placement procedures are not needed with this method. The sodium silicate gel is generally pumped into the lost-circulation zone ahead of the cement to form a barrier which retains the slurry while it sets. Unfortunately, as with the conventional Porland cement systems, difficulties arise at temperatures above 200° C [7].

The direct addition of conventional Portland cement to a highly concentrated bentonite drilling fluid produces a lower-strength material. This is considered to be due to the strongly thixotropic gel and swelling of the bentonite hydration products brought about by chemisorption of the free water in the neat cement pastes. Hence, the disadvantages of commercial cement–bentonite–water systems for utilization as CLCMs include the lack of knowledge on the actual degree of bentonite hydration, and the difficulty of mixing the thick slurry into the active mud systems. Nevertheless, the use of hydraulic cement as a sealing agent offers the following advantages; (i) wide availability, (ii) ease of direct addition to water-based drilling fluid, and (iii) relatively low cost.

The current Brookhaven National Laboratory (BNL) effort emphasized the development of cement-based sealing systems that can be added directly to the conventional water-based bentonite fluids. The goal

0022–2461/87 $03.00 + .12

was to identify cementitious sealing systems that when added to hydraulic cement will have controllable setting times and will develop adequate mechanical strength after exposure to temperatures up to 300° C. Therefore, the first part of the research was to select a retarding admixture that could be used in conjunction with the conventional cement formulations to yield a CLCM which meets the above criteria. The desired admixture would also have to be effective in improving the controllability of the bentonite hydration as well as expansion of the CLCM upon curing.

Inorganic-type admixtures, which are not susceptible to hydrothermal disintegration at high temperatures, were employed in this study. Types of materials considered included chlorine, sodium silicate, sodium phosphate, and boron compounds. The reaction products formed during autoclave exposure of the CLCM in the presence of the most suitable admixture, and the CaO–SiO_2–H_2O formations which are primarily responsible for strength developmet at elevated temperatures, were identified by means of X-ray powder diffraction (XRD) and scanning electron microscopy (SEM).

Although it is expected that a pumpable CLCM could easily penetrate into a wide size range of lost-circulation zones, it is probable that a large amount of the cementing slurry would be lost into large-sized fractures before the setting of the CLCM. Therefore, screening tests using commercially available bridging materials which were added to the CLCMs were also performed in an attempt to enhance sealing and improve the mechanical properties of the hardened plug.

2. Experimental procedure

The general properties of a standard drilling fluid consisting of 6% Wyoming bentonite (supplied by NL Baroid, Inc.) and 94% water, as measured using a Model 35A Fann Direct Indicating Viscometer, are given below:

Newtonian Viscosity (μ_n): 11.0 cP (mPa sec)

Plastic Viscosity (μ_{pv}): 6.0 cP (mPa sec)

Yield Point (YP): 5.0 lb/100 ft^2 (0.25 kg m^{-2})

μ_n was computed using the following formula:

$$\mu_n = 300 \frac{\theta}{N}$$

where θ is the Fann viscometer reading, and N (r.p.m.) is the rotation rate of the outer cylinder. μ_{pv}, which represents a fineness specification for solid dispersions in an aqueous medium, was obtained from the difference between the values of the viscometer readings at 600 and 300 r.p.m. The yield point (YP), expressed as lb/100 ft^2, represents the magnitude of clay activity created primarily by the charged surfaces and is given as follows [8]:

$$YP = \theta_{300} - \mu_{pv}$$

The value of 11.0 cP for the Newtonian viscosity, which was measured for the standard fluid, corresponds to the value specified in American Petroleum Institute (API) Standard 13A.

TABLE I Cement compositions

Cement	Composition (wt %)						Loss on ignition (wt %)
	SiO_2	CaO	Al_2O_3	Fe_2O_3	MgO	SO_3	
Class H	22.40	64.40	4.29	4.92	0.80	2.20	0.40
Class J	50.97	40.68	0.86	0.70	1.01	0.29	4.75

API Class H and Class J cements were used as the matrix for the CLCMs, since they have good strength characteristics at bottom-hole static temperatures above > 110° C. Typical chemical analyses of the Class H and Class J cements that were supplied by the Lehigh Portland Cement Company are given in Table I.

Class J is a silica–lime cement system that is not described by an API chemical specification. Unlike other API cements, Class J does not require additional silica to prevent strength retrogression at temperatures above 110° C. As a result, reactive silica flour having a particle size < 44 μm was added to only the Class H cement system. This system consisted of 60 parts cement to 40 parts silica flour.

The specimens were prepared according to the following procedures. First the bentonite fluids were thoroughly mixed with the proper amount of the various cement retarding admixtures. The Class J and Class H cement systems were then incorporated into the chemically treated fluids, and subsequently mixed using a Hamilton Beach Mixer. The CLCM mixes used in these studies were composed of 60% treated fluid, 24% cement and 16% silica flour for the Class H cement-based systems, and 60% treated fluid, 40% cement for the Class J systems. The density of both slurries was ~1.45 g cm^{-3} as determined with a Baroid Four Scale Mud Balance. On the assumption that the plugging materials will have to be placed into water-filled fractures, all the CLCM slurries were placed into water-filled test tubes and maintained at room temperature until the slurry settled completely to the bottom of the aqueous medium. After settling, the slurry-filled test tubes were exposed in an autoclave for 2 h at temperatures up to 300° C.

3. Results and discussion

3.1. Admixtures

A search was conducted to identify admixtures that would yield a slurry pumpable at elevated temperatures, which, upon curing, would have the required strength characteristics. In this work, the various inorganic chemical compounds listed in Table II were evaluated on the basis of their changes in viscosity and the thickening temperature for the CLCM slurry, and the resultant compressive strength after curing for 2 h in an autoclave at 300° C. The viscosities were measured using a Fann Direct Indicating Viscometer, Model 35A. The thickening temperature measurements were made using a stirred autoclave of diameter 7.5 cm and length 23.8 cm in a manner similar to that reported earlier [1].

The CLCM formulation employed in this series of experiments were composed of 60 parts bentonite fluid (6% bentonite–94% water) and 40 parts Class J

TABLE II Properties of 60% bentonite fluid–40% Class J cement slurry systems treated containing various admixtures

Reactive group	Admixture*	Formula	Viscosity at 300 r.p.m. (cP)	Thickening temperature (° C)	Compressive strength after exposure for 2 h in autoclave at 300° C (MPa)
–	–	–	135	160	2.27
Chloride	7.0% Aluminium chloride	$AlCl_3$	93	–	0.14
	7.0% Calcium chloride	$CaCl_2$	100	185	1.93
Phosphate	7.0% Sodium fluorophosphate	Na_2PO_4F	70	170	0.28
	7.0% Sodium phosphate	$Na_3PO_4 \cdot 12H_2O$	49	170	†
	0.5% Sodium phosphate anhydrate	Na_3PO_4	95	175	†
	1.0% Sodium phosphate anhydrate	Na_3PO_4	44	180	†
	2.0% Sodium phosphate anhydrate	Na_3PO_4	37	195	†
	3.0% Sodium phosphate anhydrate	Na_3PO_4	36	210	†
	5.0% Sodium phosphate anhydrate	Na_3PO_4	35	250	†
	7.0% Sodium phosphate anhydrate	Na_3PO_4	35	> 300	†
Boron	7.0% Sodium tetraborate decahydrate (borax 10 mol)	$Na_2B_4O_7 \cdot 10H_2O$	70	280	1.93
	10.0% Sodium tetraborate decahydrate (borax 10 mol)	$Na_2B_4O_7 \cdot 10H_2O$	55	280	1.72
	7.0% Sodium tetraborate pentahydrate (borax 5 mol)	$Na_2B_4O_7 \cdot 5H_2O$	62	230	1.79
	7.0% Sodium tetraborate anhydrous (anhydrous borax)	$Na_2B_4O_7$	65	200	1.65
	0.5% Boric acid	H_3BO_3	110	210	†
	1.0% Boric acid	H_3BO_3	94	240	†
	2.0% Boric acid	H_3BO_3	81	> 300	†
Other	7.0% Sodium silicate	$Na_2SiO_3 \cdot 9H_2O$	80	–	0.14
	7.0% Barium sulphate	$BaSO_4$	112	180	2.27

*Percentage by weight of bentonite–cement mix slurry.
†Too low to be measured.

cement. The admixtures were added directly to the bentonite mud before mixing the Class J cement. It should be noted that all reported admixture concentrations are by weight of the bentonite–cement mix slurry. All the chemical agents were supplied by the Fisher Scientific Co., except for the commercial-grade boron compounds, which were obtained from the United States Borax Chemical Corporation.

Data from this series of tests are summarized in Table II. In the absence of any admixtures, the control slurries had a viscosity of 135 cP (mPa sec), a thickening temperature of ~160° C, and a compressive strength of 2.27 MPa at an age of 2 h. The relatively high viscosity results in the formation of a thixotropic gel of bentonite hydration caused by chemisorbing the water in the neat cement pastes. As a result, the onset of setting is at the relatively low value of ~160° C. The data also indicate that the addition of admixtures which are soluble in the alkaline bentonite fluid reduces the viscosity and increases the thickening temperature of the slurries. All the admixtures used in this study appear to be hydrolysed by the alkaline solution to dissociate uni-, di-, and trivalent ions, and these ions act to inhibit the rates of bentonite and cement hydration. It appears from the data that univalent cations such as Na^+ and H^+ are more effective in reducing the slurry consistency at 24° C than are the di- and trivalent cations such as Ca^{2+}, Ba^{2+} and Al^{3+}. For example, slurries containing $AlCl_3$ and $CaCl_2$ had viscosities ranging from 93 to 100 cP, while those containing sodium phosphate, sodium borate compounds and boric acid had values from 70 to 35 cP. Of the various univalent cation-dissociating admixtures tested, sodium phosphate anhydrate (Na_3PO_4) was the most effective in reducing the viscosity of the control slurry. With a 5% concentration of Na_3PO_4, the viscosity was 35 cP, ~74% less than that of the control. Slurry viscosities ranging between 70 and 62 cP can be obtained by adding a 7% concentration of anhydrous and hydrated sodium tetraborate reagents.

The thickening temperature for the slurries is also dramatically raised with an increase in the Na_3PO_4 admixture concentration. The thickening temperature of the control was extended to > 300° C by the addition of 7% Na_3PO_4, but unfortunately the 2 h compressive strength for the cured formulation was too low to be measured. Reducing the Na_3PO_4 concentration to 0.5% did not result in strength improvements. Similar results were obtained from specimens containing the boric acid admixture. It is speculated that Na_3PO_4 and H_3BO_3 admixtures which liberate large numbers of PO_4^{3-} and BO_3^{3-} ions as the counterions of Na^+ and H^+ indefinitely retard the setting and hardening of hydraulic cement at temperatures up to 300° C.

The best admixtures for retarding the hydration of the cement but yet meeting the early strength criteria were the borax compounds such as borax 10 mol, borax 5 mol, and anhydrous borax. Of these various borax additives, the borax 10 mol gave the greatest enhancement in thickening temperatures and compressive strength. Specimens containing 7% of the borax 10 mol exhibited a thickening temperature of

280° C, 120° C over that of the control, and the autoclaved specimens had a 2 h strength of 1.93 MPa. A further increase in the borax concentration up to 10% resulted in an appreciable strength reduction.

The ability of Na^+ and $B_4O_7^{2-}$ ions released by dissolution of the borax 10 mol to improve the controllability of the hydration distribution of bentonite–cement composite systems is of particular interest. Since the borax admixtures were usually added to the bentonite fluids before mixing the cement, the chemical affinity between the dissociated ions and the bentonite muds was studied first. Reasons for these ions acting to retard the hardening rate of the cements were then investigated. The experimental work was performed in accordance with the following procedures: 100 g of the bentonite fluid were placed in a 300 ml glass beaker and 7 g of the borax 10 mol were then added to the fluid. The beaker was then sealed and the fluids were mixed at room temperature for up to 24 h. The aqueous phase was then extracted by a centrifugal separation. Concentrations of Na^+, $B_4O_7^{2-}$ and silicate ions in the extracted liquids were then determined using atomic absorption spectrophotometry (AA) and high-performance anion chromatography (HAC). X-ray powder diffraction analyses (XRD) with Cu$K\alpha$ radiation were also performed on treated bentonite fluids that were exposed in the autoclave at 300° C for 2 h, and then dried. These data yield information regarding the reaction products formed by the autoclaving.

As shown in Fig. 1, the amount of Na^+ ions in solution increases with mixing time until the concentration reaches a peak value of $\sim 4.3 \times 10^{-1}$ M after ~ 300 min. The concentration then decreases gradually to $\sim 3.5 \times 10^{-1}$ M after 1440 min. In contrast, the $B_4O_7^{2-}$ reached a maximum concentration of $\sim 1.9 \times 10^{-1}$ M within ~ 300 min and then remained constant. This implies that the fluids became saturated with both ions during a mixing period of ~ 300 min. In contrast the concentration of silicate ions dissociated from the montmorillonite tends to increase with elapsed time, ranging from 4.5×10^{-4} M after 10 min to 3.1×10^{-3} M after 1440 min. These values are approximately two orders of magnitude less than those for Na^+ and $B_4O_7^{2-}$.

The structure of anhydrous montmorillonite, which consists of an $[Al_2(OH)_4]_n^{2n+}$ sheet layer sandwiched between two $(Si_2O_5)_n^{2n-}$ sheet layers, is composed of superposed lamellae which have an edge absorption at a diffuse negative silica sheet with various cations balancing unsaturated oxygen ions at the edges of the crystal lattice of the lamellae. It is well known [9–11] that the negative charge arising on this layer as the result of the substitution is balanced by chemisorption of cations such as H^+, Na^+, K^+, Ca^{2+}, Mg^{2+} and Al^{3+} ions located between the sheets together with molecules of water. The XRD patterns of the dried borax treatment montmorillonites were characterized by strong lines at 1.77, 0.441 and 0.329 nm, and medium intensities at 0.358 and 0.311 nm. These spacings can be ascribed to the sodium-saturated montmorillonite hydrate formed by hydrothermal reactions between the negatively charged silicate

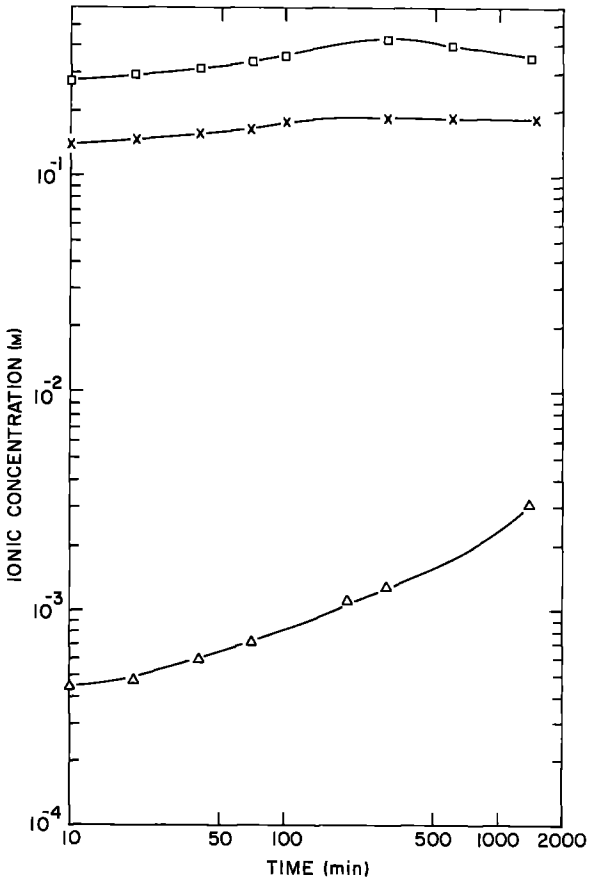

Figure 1 Changes in concentration of Na^+, $B_4O_7^{2-}$ and silicate ions in the liquid phase of bentonite fluids mixed with borax. (□) Na^+, (×) $B_4O_7^{2-}$, (△) Si.

plates of montmorillonite and the Na^+ ions liberated from the borax [12]. The Na^+ ions are more likely to be chemisorbed on to the cation-absorbing silicate surface of montmorillonite by proceeding to neutralization, rather than to the dissolved silicate ions. The $B_4O_7^{2-}$ ions which are substantially inert to $Si–O^-$ surfaces remain as a reactive ion species in the bentonite fluids.

On the basis of the above experiments, it is possible to speculate on possible interaction mechanisms between the Na^+ ions and the hydrated montmorillonite sheet layers as follows: when the bentonite powder is mixed with water, the diffuse negative silica sheets at the edges of the montmorillonite crystal lattice strongly chemisorb large numbers of water molecules to initiate the hydration of bentonite. Simultaneously, silicate ions are released from the montmorillonite surfaces. This separation between the clay plates that is brought about by water adsorption of bentonite plays an essential role in increasing the fluid viscosity, resulting in the swelling of the bentonite. Both the Na^+ and $B_4O_7^{2-}$ ions dissociate immediately after the addition of the borax to the hydrated bentonite fluids, and the maximum concentrations of these ions in the fluids occur within ~ 300 min. Subsequently the Na^+, which can be expressed in terms of the compensation ions, is chemisorbed on the $Si–O^-$ located between the intersheets. Once the negative silica sheets are neutrally balanced by the compensative Na^+ ions, the water-

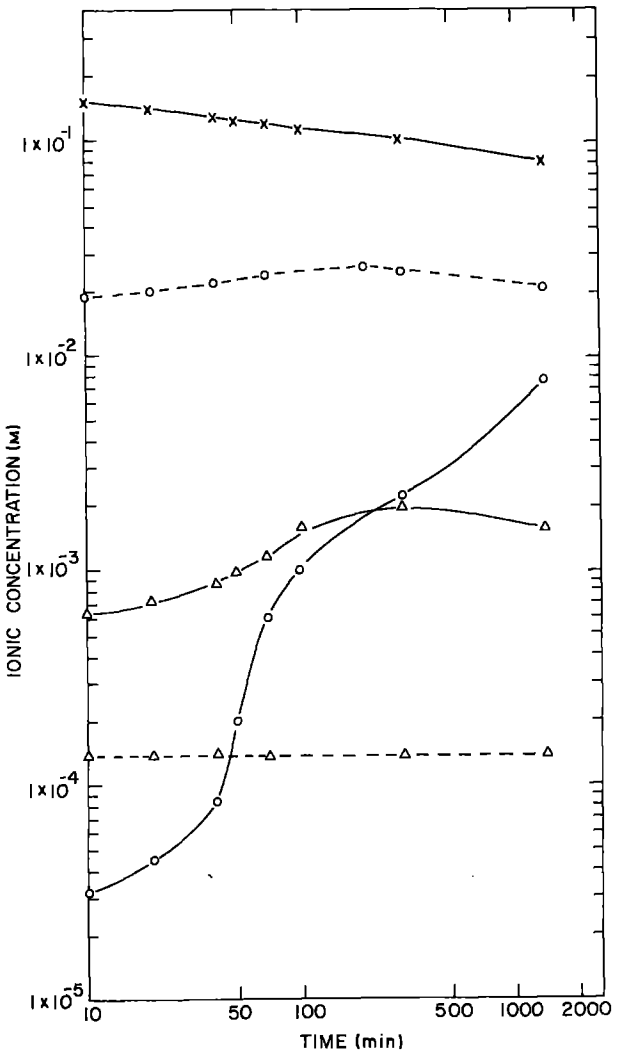

Figure 2 Ionic concentration in the extracted liquid of (---) cement paste and (——) borax-treated bentonite fluid containing cement. (×) $B_4O_7^{2-}$, (○) Ca^{2+}, (△) Si.

adsorbing capacity of the interlayers becomes very small. These Na^+ ion-saturated intersheets lead directly to reductions in the consistency of the bentonite fluid as a result of the reduced swelling of the bentonite. Hence, when hydraulic cement is introduced into the neutralized bentonite particles, the rate of thixotropic gel formation of the bentonite fluid caused by chemisorption of the water existing in the neat cement pastes is considerably lower.

On the other hand, the effect of $B_4O_7^{2-}$ ions on the retardation of setting cement was studied on the basis of results from slurry samples prepared by mixing Class J cement with the borax-treated bentonite fluid. For the analysis of Ca^{2+}, $B_4O_7^{2-}$ and silicate ions at a given mixing time, the aqueous phase was extracted using a centrifugal separator, and the concentration of these ions was then determined using AA and HAC. The bentonite–cement mix slurries contained a treated bentonite fluid/cement ratio of 3.06. For purposes of comparison with the changes in the dissociated Ca^{2+} and silicate ions in the bentonite–borax–cement–water systems, ionic concentration analyses of ordinary Class J cement pastes having a water/cement ratio of 2.69 were also performed.

The analysed results for dissolved Ca^{2+}, $B_4O_7^{2-}$ and silicate ions from these material systems are shown in Fig. 2. In the liquid phase of neat cement pastes, the concentration of Ca^{2+} increases with stirring time until a concentration of $\sim 2.6 \times 10^{-2}$ M is reached after 200 min. After that it decreases slowly. The quantitative level of silicate ions dissociated from the cement is extremely low, typically two orders of magnitude less than that of Ca^{2+}. The observation is in agreement with the results given by several other investigators [13–15].

Compared to the Ca^{2+} or silicon concentration against stirring time relation for the cement paste systems, very different curves were obtained for the bentonite–borax–cement–water slurry systems. For example, the Ca^{2+} ion concentration in the aqueous phase of the cement–bentonite slurry systems was only 3.2×10^{-5} M after 10 min. This is approximately three orders of magnitude lower than that for the cement paste systems. This extremely low level of Ca^{2+} dissolution in the induction period for cement hydration is probably due to a rapid adsorption of $B_4O_7^{2-}$ counterions by the Ca^{2+} ions which form the positively charged surface of hydrating cement grains. The concentration of $B_4O_7^{2-}$ ions with time, therefore, tends to decrease as the concentration of Ca^{2+} ions increases. The quantity of silicate ions should be the sum of the ions dissolved from the bentonite (see Fig. 1) and the cement grains (shown in Fig. 2). However, the values between 10 and 300 min are appreciably higher than the sum of values obtained from the individual cement paste and bentonite–borax fluid systems. Although there is some discrepancy in the total quantity of soluble silicate species, the curve indicates that the silicate ions reach a peak concentration of 2.0×10^{-3} M after a stirring time of 300 min, and then drops to 1.6×10^{-3} M after 1440 min.

In an attempt to develop a correlation between the Ca^{2+}, $B_4O_7^{2-}$ and silicate ion dissolutions, the changes in viscosity and pH of the slurry samples were plotted against the stirring time. As seen in Fig. 3, the viscosity

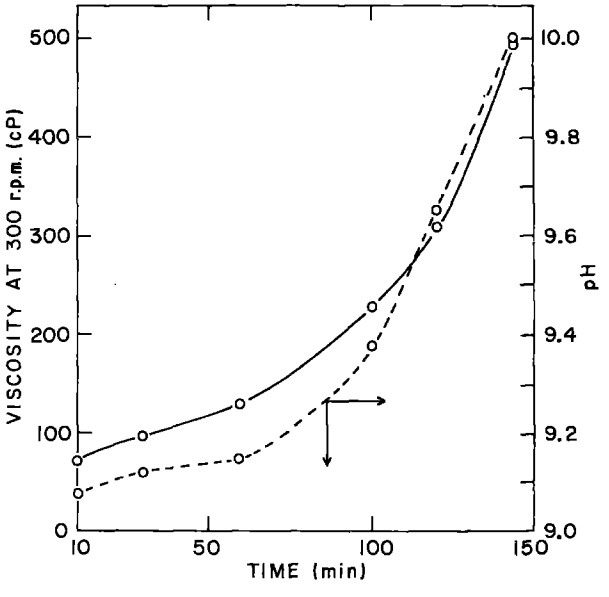

Figure 3 Variations in viscosity and pH of bentonite–borax–cement–water slurry systems as a function of stirring time.

of the slurry increases gradually for ~100 min after the cement is added to the borax-treated bentonite fluids, and then rapidly rises. Similar trends were obtained for the pH values. The rapid increase in viscosity and pH after ~100 min is due to the increased precipitation of colloidal calcium silicate hydrate (CSH) formed in the vicinity of the cement grains. This would be associated with the previously discussed peak concentration of silicate ions after ~300 min.

From the above information, a possible explanation for the retarding activity of $B_4O_7^{2-}$ ions is as follows: when mixed with bentonite fluid, borax appears to be hydrolysed by the alkaline solution to liberate $B_4O_7^{2-}$ ions which act as Ca^{2+} cation-accepting anions. After the addition of cement powder, the $B_4O_7^{2-}$ ions react rapidly with Ca^{2+} ions relesed from the cement grains in the colloidal bentonite–borax–cement–water phase. This reaction with Ca^{2+} ions results in the precipitation of a calcium-depleted silica gel and the conversion into a semipervious film of Ca^{2+}–$B_4O_7^{2-}$ compounds covering the cement grain surfaces. Although the cement-retarding mechanisms are due to either the precipitation or the conversion membrane coating, these effects are thought to delay the nucleation processes of C–S–H gel formation and to provide an effective barrier to the further hydration reaction between the cement and water until it is gradually destroyed by calcium dissociated from the cement paste. The precipitation of a colloidal C–S–H gel produced by the ionic reaction between the Ca^{2+} in solution and the hydrolysed silicate-rich surface of the cement grains is likely to begin after ~100 min hydration. It appears that the hydrolysed products of borax have a moderate ability to bind the calcium ions in alkaline bentonite fluids.

Consequently, the borax 10 mol admixture appears to have a high potential for use as an inhibitor for both the bentonite and the cement hydration in these specific CLCM systems. The key element governing the retarding functions was found to be hydrolytically degraded products of the borax.

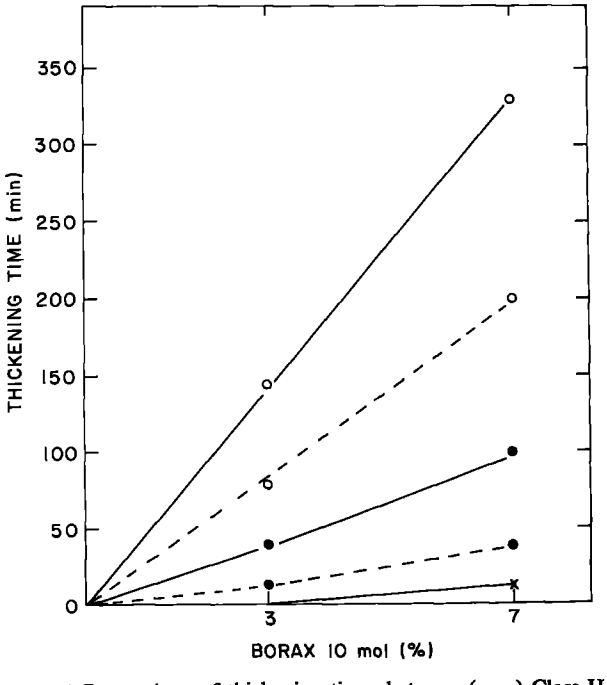

Figure 4 Comparison of thickening times between (——) Class H and (– – –) Class J cement systems treated with borax at isothermal temperatures of (○) 200, (●) 250 and (×) 300° C.

Further information regarding the ability of borax to retard the setting of cement is given in Fig. 4. Data for the thickening time of bentonite–cement–water slurry systems as a function of temperature and borax concentration are given. The major aim in this test was to gain information regarding the actual workability of the bentonite–borax–water Class H and Class J cement systems at hydrothermal temperatures of 200, 250 and 300° C, under a pressure of 10.34 MPa. At 200° C, the lowest temperature investigated, the thickening time for non-borax-containing bentonite Class H or J slurry systems was too short to be measured. The workability of the Class H and Class J systems was dramatically extended to ~145 min and ~80 min, respectively, by the addition of 3% borax. A further increase in borax concentration to 7% extended the thickening times for both systems to ⩾ 200 min. Similar trends were noted for slurry specimens at 250 and 300° C. However, at a temperature of 300° C, the workability of the Class J system containing 7% borax could not be measured because of the rapid hardening.

It is also evident from Fig. 4 that the thickening times for the borax-treated Class H systems are longer than for the Class J systems. Thus, the proper choice of cement is likely to be one of the key factors associated with extending the thickening times for CLCMs. Since the CLCMs must be capable of safely accommodating interruptions in pumping operations due to mechanical trouble, or if regions of unpredictably high geothermal temperature are encountered, it is assumed that the required thickening times should be at least 100 min. For the Class H systems in the 200 to 250° C range, the addition of ~7.0% borax meets this criterion. Unfortunately, at 300° C the thickening time was only ~15 min. Therefore, further work in which the borax-based composite system is used in conjunction with other boron-type reagents is necessary before the CLCM can be considered for placement at temperatures ⩾ 300° C.

It was also found that the borax is effective as a swelling agent. Although it is not shown in the figures or the tables, the linear expansion increased with the amount of borax up to a concentration of 7%. Specimens without borax exhibited a shrinkage of ~1.6% after exposure for 2 h at 300° C. Formulations containing 3% and 7% borax showed expansions of ~1.9% and ~2.2%, respectively. This slight expansion characteristic might help to yield an effective seal after placement.

3.2. Effect of C–S–H on compressive strength and water permeability

Tests were performed to determine if changes in the compressive strength and water permeability of borax-modified CLCMs occur upon continued exposure in an autoclave. In this work, bentonite Class H and Class J slurry systems containing 7% borax were cast into glass tubes of diameter 3.5 cm and length 7.0 cm

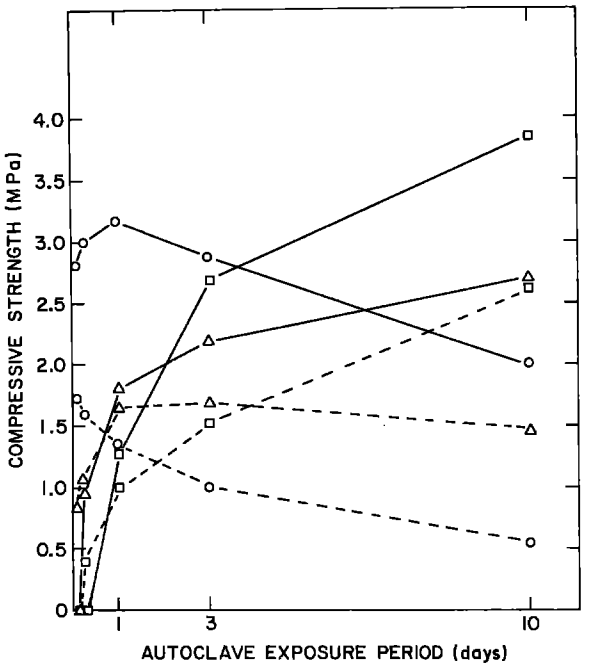

Figure 5 Changes in compressive strength of 7% borax-modified CLCMs as a function of exposure times at isothermal temperatures of (○) 300, (△) 250 and (□) 200° C. (——) Class H cement system, (– – –) Class J cement system.

for use in compressive strength meausrements, and in 3.0 cm × 4.0 cm tubes for water permeability tests. The specimens were then exposed in an autoclave for up to 10 days at temperatures of 200, 250 and 300° C. The data were then correlated with the phase analyses of reaction products identified using XRD and the morphological features of the crystal forms using scanning electron microscopy (SEM).

The compressive strength and water permeability results are shown in Figs 5 and 6, respectively. Phases detected by XRD in several specimens are summarized in Table III. It was found that at 300° C the compressive strength of Class H cement composites increased with exposure time up to ~24 h. At this age, a strength of 3.3 MPa was developed. Continued autoclave exposure resulted in strength reductions. The water permeability exhibited an initial decrease, reaching a minimum at ~6 h. It then gradually increased. However, after 10 days the permeability was still at a satisfactory value of 5.7×10^{-4} Darcys.

The results from XRD analyses revealed dramatic changes in the phases of the C–S–H compounds formed as a function of the autoclave exposure time. The hydration products formed within the first two hours were primarily 1.1 nm tobermorite, $Ca_5(Si_6O_{18}H_2) \cdot 4H_2O$. Truscottite, $Ca_{14}Si_{24}O_{58}(OH)_8 \cdot 2H_2O$ in conjunction with a small amount of xonotlite, $Ca_6Si_6O_{17}(OH)_2$, was present as the major crystalline product after a 10-day exposure to the hydrothermal environment. Electron micrographs of fractured surfaces of 2 h and 10 day specimens are shown in Figs 7 and 8, respectively. In Fig. 7 it can be seen that the morphology of the tobermorite yielded from a CLCM formulation composed of 56% bentonite fluid, 4% borax, 24% Class H cement and 16% silica flour after exposure for 2 h at 300° C is characterized by an interlocking structure of fine fibrous crystals. In contrast, the microcrystalline feature of the mixture of truscottite and xonotlite produced during the 10-day autoclave exposure is an intermixture of fibrous plates and fine needles. The former are present in the form of truscottite crystals. The transformation of tobermorite into xonotlite and subsequently into truscottite yields an excess of silica and water at the elevated temperatures. These phase changes can be deduced from the pronounced reduction of the line intensity at 0.334 nm spacing which is ascribed to the presence of unreactive silica. The silica remaining in the samples is very reactive and forms truscottite. Despite the work by Luke and Taylor [16], there does appear to be transformation of xonotlite into truscottite. However, the xonotlite–truscottite transformation was still incomplete after a 10-day exposure. The formation to truscottite in the hardened CLCM seems to result in a strength decrease and enhanced water permeability. Truscottite, therefore, is a low-strength binder. In contrast, a well-crystallized tobermorite formation would yield improvements in strength and a decrease in permeability. A xonotlite binder would be likely to yield properties intermediate between those of the tobermorite and truscottite. The observed strength decrease and permeability increase in the cementitious

TABLE III $CaO–SiO_2–H_2O$ phase assemblages crystallizing in bentonite–Class H and Class J cement sytems as a function of autoclaving temperatures and time

Cement Class	Temperature (° C)	Time (h)	Phases present	
			Major	Minor
H	300	2	1.1 nm tobermorite + quartz	–
	300	24	1.1 nm tobermorite + xonotlite + quartz	–
	300	240	Truscottite	Xonotlite + quartz
	250	24	1.1 nm tobermorite + quartz	Xonotlite
	250	240	Xonotlite + quartz	1.1 nm tobermorite + truscottite
	200	72	1.1 nm tobermorite + quartz	–
	200	240	1.1 nm tobermorite	Quartz
J	300	2	1.1 nm tobermorite + xonotlite	Quartz + scawtite
	300	72	Truscottite	Xonotlite + scawtite + quartz
	300	240	Truscottite	Xonotlite + scawtite
	250	24	Xonotlite + quartz	–
	250	240	Truscottite + xonotlite	Scawtite
	200	24	1.1 nm tobermorite + scawtite + quartz	–
	200	240	1.1 nm tobermorite	Scawtite + quartz

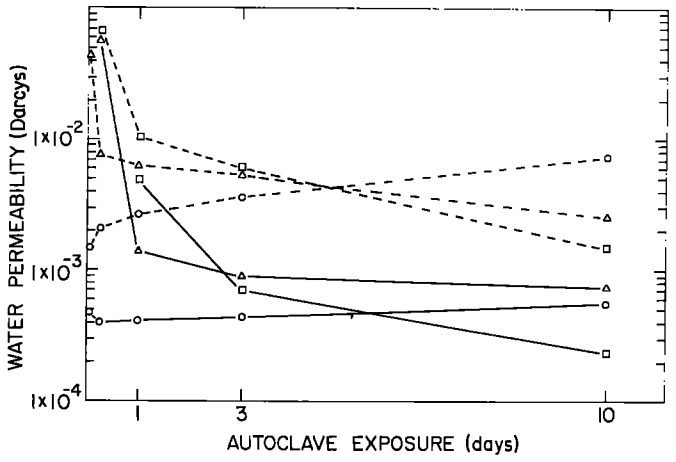

Figure 6 Water permeability of CLCMs containing 7% borax as a function of exposure time at (○) 300, (△) 250 and (□) 200° C. (——) Class H cement system, (– – –) Class J cement system.

materials caused by the formation of truscottite are in agreement with results published by other authors [17, 18].

Specimens autoclaved at 200 and 250° C exhibited progressive increases in strength with ageing times of up to 10 days. However, the 250° C 2 h and 200° C 6 h specimens did not develop sufficient strength to be measured. This was due to the remarkable retarding ability of the borax. The 200° C 10-day specimens developed a strength of 3.8 MPa, the highest for all of the specimens tested thus far. They also yielded the lowest permeability values.

As expected, XRD data for the 250° C aged samples indicated that tobermorite and silica were the major constituents after a one-day exposure. After a 10-day exposure, xonotlite and silica were present as the major phase in conjunction with tobermorite and truscottite as minor products. The recrystallization from xonotlite to truscottite at 250° C was apparently much slower than for the samples at 300° C. Thus, continued strength development could be anticipated by further autoclave curing. The XRD patterns at 200° C showed that the tobermorite formed during the 72 h exposure was converted into well-crystallized tobermorite formulations after 10 days of autoclaving. This binder appears to result in the high magnitude of strength development.

For the CLCM containing Class J cement at 300° C, the strength within the first 2 h of autoclaving decreased gradually with increased exposure time. The strength of ~0.5 MPA for the 10-day aged specimens corresponds to a reduction of ~71%, as compared to that for the 2 h autoclaved specimens. For the latter, the predominant reaction products were found to be a mixture of tobermorite and xonotlite in the presence of the unreactive silica as a minor phase. Extended autoclave time tended to favour the formation of truscottite. Xonotlite–truscottite transformation is likely to occur progressively during exposure periods of ~72 h, and simultaneously forms a small amount of scawtite, $Ca_7Si_6(CO_3)O_{18} \cdot 2H_2O$. This can be detected by the noteworthy decreases in the peak intensities at 0.308 and 0.334 nm spacings which represent the xonotlite and silica, respectively, and the growth of a new peak at ~0.300 nm which is representative of the formation of scawtite. Since scawtite contains a small amount of CO_2 in its molecular structure, the formation is associated with the presence of CO_2 in cements [19]. Extending the exposure time to 10 days results in an increase in the conversion rate to truscottite rather than xonotlite.

Fig. 9 shows scroll-tubular crystals of truscottite produced from a mixture of 56% bentonite fluid, 4% borax and 40% Class J cement after 10 days at

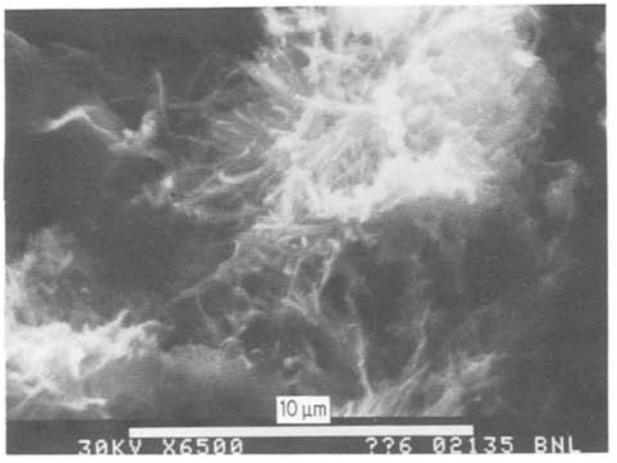

Figure 7 Electron micrograph of tobermorite formed in 2 h at 300° C from bentonite–borax–class H cement–silica flour–water systems.

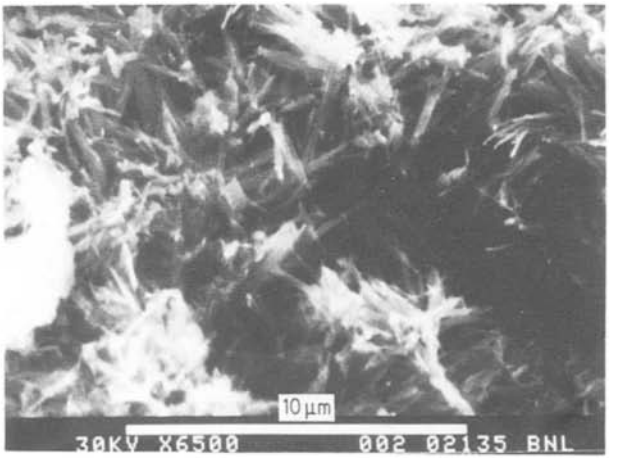

Figure 8 Fibrous plates of truscottite blended with fine needles of xonotlite produced from Class H systems autoclaved at 300° C for 10 days.

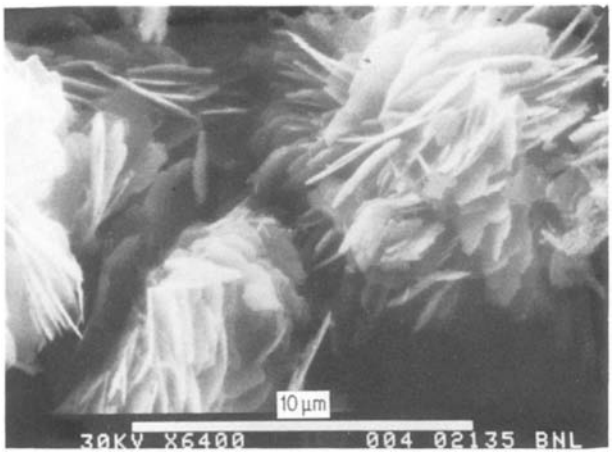

Figure 9 Scroll-tubular crystals of truscottite formed in 10 days at 300° C from bentonite–borax–Class J cement–water systems.

300° C. From the standpoint of the space-filling characteristics and morphological features of the microcrystalline forms, the truscottite structure produced from Class J cement can be categorized as a porous binder in the form of thin plates ~5 µm in length, and is an inferior binder to that produced from Class H. The low density of the crystal formations relates directly to poor strength development and high water permeability. Again, an increase in the quantity of truscottite in the systems results in increased water permeability. At 250° C, an increase in strength was noted over exposure periods ranging from 2 to 24 h. Further exposures up to 3 days had little effect on strength, which remained at ~1.7 MPa. Specimens tested after exposure for 10 days exhibited appreciable reductions in strength, due mainly to the formation of truscottite.

As discussed earlier, the major reaction products of Class H and Class J systems at the same temperature and age are, respectively, xonotlite and truscottite. It appears that the xonotlite–truscottite transformation processes in Class J systems are much faster than those in Class H systems containing a large amount of silica flour. In the manufacture of commercially available Class J cement, reactive silica is added to the cement. Therefore, the differences between the transformation rates in Class H and Class J systems may account for the characteristics of crystallinity, surface area, particle size, and concentration of silica added to cement.

As is evident from the decrease in permeability of samples autoclaved at 200 and 250° C (see Fig. 6), the Class J CLCM slurries were converted into high-density cements during exposure for up to 10 days in the autoclave. The basal spacings of 200° C 10-day aged specimens revealed the presence of a large amount of a well-crystallized tobermorite and very small amounts of scawtite and silica.

The above results suggest that the major factors determining the quality of the hardened CLCMs depend primarily on the C–S–H species formed under the hydrothermal conditions. The phase transformations of C–S–H groups produced in these particular CLCM systems over temperatures ranging from 200 to 300° C for 10 days are estimated to be in the order of tobermorite > xonotlite > scawtite and truscottite. The strength retrogression and permeability increase which occur gradually during the 10-day exposure at 300° C, therefore, were rationalized to be due to the transformation from tobermorite to xonotlite and from xonotlite to truscottite.

3.3. Bridging additives

Although small-fracture lost-circulation zones might be satisfactorily sealed using non-particulate-containing CLCM plugging materials, it is also necessary to address the problem of sealing large fractures. To solve this important problem, the ability of commercially available bridging materials used in conjunction with the CLCM formulations to plug various size fractures was estimated. In these studies compressive strength and slot tests, using an American Petroleum Institute (API) lost-circulation test cell that had been modified by Sandia National Laboratory, were undertaken to evaluate six bridging materials: fibreglass, Wallnut (crushed granular nuthulls), Fibertex (processed can fibres), Micatex (crushed miscovite mica flakes), Flug-git (shredded hardwood fibre) and Hy-seal (shredded organic fibre). The first series of screening tests consisted of compressive strength measurements for CLCMs containing the various additives after exposure in an autoclave for 24 h at 300° C. These test results provide information on the hydrothermal stability of the bridging materials in strong alkaline environments and their ability to enhance the mechanical properties of the CLCMs at an early autoclaving age.

The specimens used contained various concentrations of bridging additives in a CLCM formulation consisting of 56% bentonite fluid, 4% borax, 24% Class H cement and 16% silica flour. The fibreglass (supplied by Owen-Corning Fiberglass Corp.) was 6.25 mm long, and contained a chopped E-type glass. This type of glass generally disintegrates in strong alkalis at boiling temperature [20]. All the other additives were obtained from NL Barold Industries, Inc.

The compressive strengths of 300° C 2 h aged specimens as a function of bridging material concentration are shown in Fig. 10. As seen in the figure, the strengths of the hardened CLCMs depend primarily on the type and concentration of the particulates added to the CLCM. The highest strength obtained in this test series (3.7 MPa) was achieved by adding ~0.2% fibreglass, which represents an improvement of ~76% over that of the specimens without bridging materials. Further increases in the concentration of fibreglass resulted in strength reductions, probably due to poor compaction of the CLCM as a result of the increased slurry viscosity. Similar trends were obtained with the Wallnut- and Fibertex-containing CLCMs. The other bridging additives evaluated did not produce strength increases, and are therefore considered unsuitable. From these initial tests, it was concluded that fibreglass is the additive most effective in improving the mechanical properties of the autoclaved CLCMs.

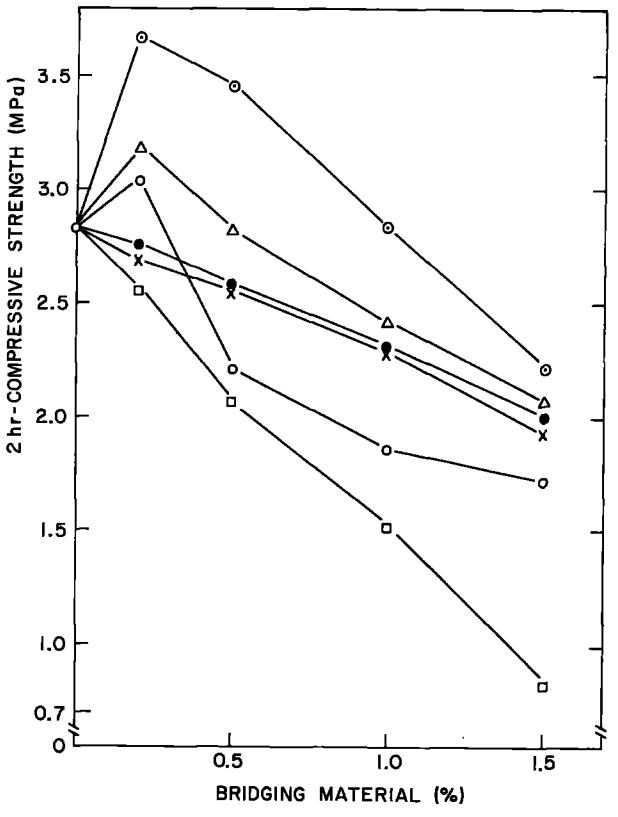

Figure 10 Changes in compressive strength of 300° C 2 h specimens as a function of concentration of various bridging additives. (⊙) Fibreglass,)△) Wallnut, (○) Fibretex, (●) Micatex, (×) Plug-git, (□) Hy-seal.

As mentioned earlier, the fibreglass used is susceptible to chemical decomposition in strong alkaline media. Thus, it was anticipated that exposure of the fibreglass-containing CLCM in an autoclave at 300° C would result in rapid deterioration of the mechanical properties because of disintegration of the fibreglass due to the alkaline nature of the matrix. To study the rate of deterioration, samples containing 0.5% fibreglass were exposed in the autoclave for up to 7 days at 300° C. For comparison, control specimens were also examined.

The test results are listed in Table IV. An unexpected result was noted for the bridged specimens, namely, their strength as a function of exposure time was almost equal to that for the controls. The strengths for both materials increased within the first 24 h, and then decreased slowly. After exposure for 7 days, the strength of the bridged specimen was 2.89 MPa, ~ 16% less than that of the 2 h-aged specimens. The controls showed a similar reduction.

XRD analyses of the specimens were performed to identify the reaction products. The results for both the unbridged and bridged CLCMs indicated the presence of tobermorite as a major phase within the first 2 h and a mixture of xonotlite, tobermorite, and truscottite after 7 days. The quantities of these hydration products in the bridged CLCMs were found to be approximately equal to those in the controls. This proves that the decrease in strength of the bridged specimens is due mainly to the phase transformation of C–S–H products rather than to the alkaline degradation of the fibreglass.

The energy-dispersive X-ray (EDX) spectrometer coupled with SEM was used to study the morphological features and chemical compositions of the fibreglass surfaces after exposure to $Ca(OH)_2$-oversaturated solutions for 24 h at 300° C. Fig. 11 shows the microstructures and selected element counts of the fibre surfaces before and after exposure to the hot $Ca(OH)_2$ solutions. The abscissa of the spectrum is the X-ray energy characteristic of the element present, and the intensity of a gross peak count is related directly to the amount of each element present. The fibreglass before exposure discloses a smooth surface nature, and the predominant element as shown in the EDX spectrum is the silicon atom. Dramatic changes in the surface morphology of the fibre were observed on the samples exposed to the $Ca(OH)_2$ solution. From Fig. 11c, the surface was characterized by a microstructure consisting of fine needle-like crystals resembling tobermorite and xonotlite precipitated on the fibre surfaces. EDX (Fig. 11d) showed that the count intensity of silicon was appreciably lower than that of calcium. In addition, AA analysis of the strong alkaline solution after removal of the fibre indicated the presence of a large amount of silicate ions which were dissolved by alkaline degradation of the fibres. It is inferred that the silicate ions dissociated from the fibre surfaces react with Ca^{2+} ions in $Ca(OH)_2$-saturated aqueous media. This hydrothermal reaction leads to the precipitation of C–S–H compounds in the vicinity of the fibre surface. The precipitated reaction product was identified using XRD. The resulting X-ray lines could belong to the C–S–H phase which is known to form with a needle habit. The basal spacings at 0.309, 0.298 ad 0.285 nm are ascribed to the possibility of the presence of tobermorite. When the fibre surfaces are completely covered with the well-crystallized tobermorite formations, the precipitated crystal layer may act as a protective layer which prevents the further alkaline disintegration of the fibres. Further work will be needed to study in detail the interfacial nature and the bonding behaviour between the precipitated crystals and the fibreglass. Nevertheless, the formed crystals serve a crosslinking function to connect the hydrated cement and the fibre. The bond strength at the cement matrix–fibre interfaces can be predicted to be at least as good as the strength of the crystals themselves. However, the

TABLE IV Comparison of compressive strength between unbridged and fibreglass-bridged CLCMs as a function of autoclaving age at 300° C

Material	Compressive strength (MPa) after exposure in autoclave at 300° C			
	2 h	1 day	3 days	7 days
Unbridged CLCM	2.80	3.18	2.88	2.35
Glassfibre-bridged CLCM	3.46	3.95	3.30	2.89

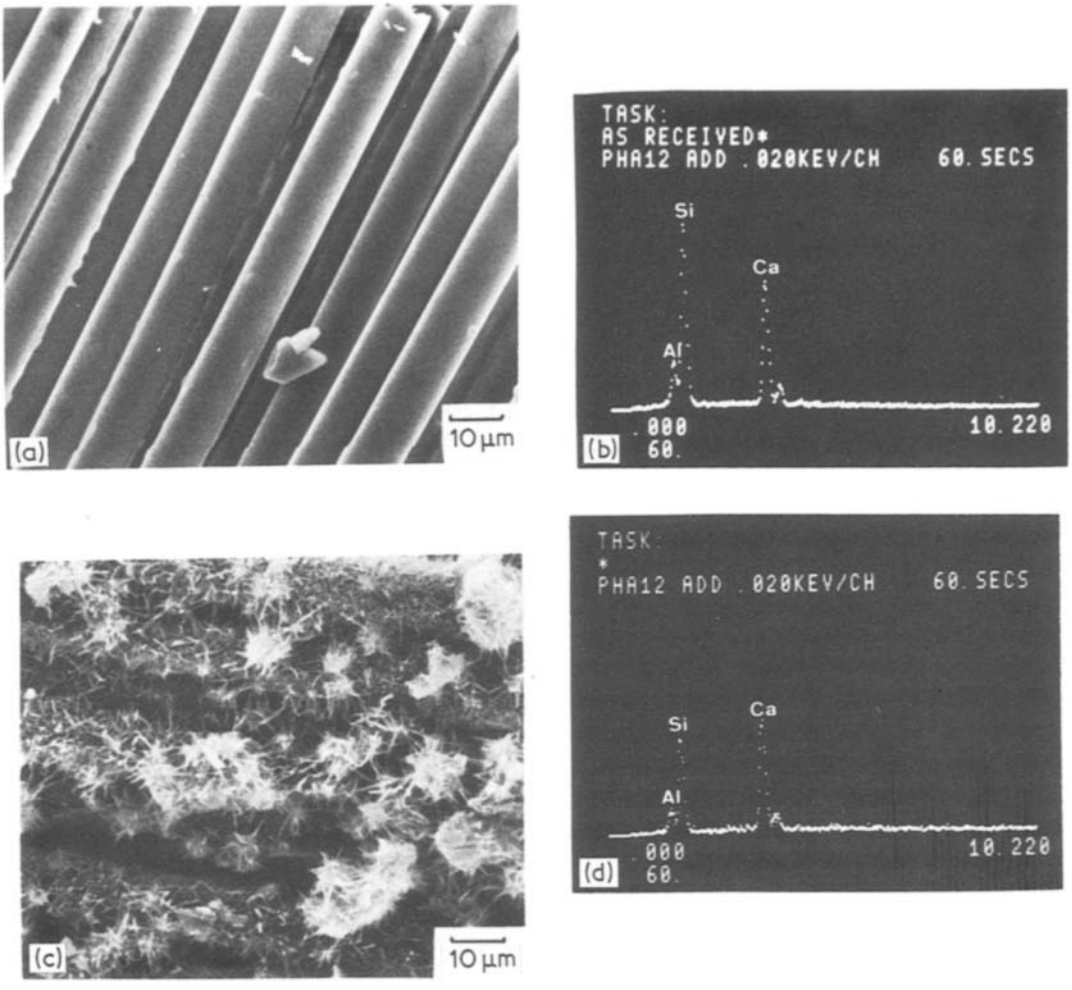

Figure 11 SEM micrographs and EDX spectra of fibreglass surfaces (a, b) before and (c, d) after exposure to a $Ca(OH)_2$ solution for 24 h at 300° C.

interfacial shear strength is high because of the large solid matrix–fibre contact area.

3.4. Slot tests

Since the maximum sealing pressures are observed to be highly variable, it is desirable to view these pressures relative to those that will actually occur in the wellbore. The wellbore pressure will have several components associated with it. The difference between the hydrostatic fluid head of the drilling fluid and the formation pore pressure is > 3.45 MPa for many geothermal formations which are typically underpressured. The dynamic pressure associated with the fluid surge when the drill pipe is run into the hole is also of the order of 3.45 MPa so that downhole pressures that are 6.89 MPa greater than the formation pressure are not uncommon. Hence, for a lost-circulation material to be useful in geothermal formations, it must be capable of sealing 6.89 MPa in the modified API tester [21].

Using the above information, slot tests were performed at room temperature to provide preliminary data regarding the ability of fibre glass to plug fractures of various sizes. In these tests, slots 150 mm long were used in place of the standard API slots. As a result of the screening tests described earlier, the one bridging material evaluated in this test series was the 6.25 mm-long chopped fibreglass. The concentration was varied in the range of 1 to 5%. Test procedures were as follows. With the outlet valve closed and a slot of specified width in place, 3500 ml of the fibre–mud mixture were poured into the reservoir. A piston to separate nitrogen driving pressure from the drilling fluid mixture was then emplaced. The cap was then screwed on to the reservoir and the outlet valve was opened. With only hydrostatic pressure acting, the amount of fluid passing was recorded. The pressure on the fibre–mud slurry was then gradually increased at a rate of ~ 0.03 MPa sec^{-1} until 6.89 MPa was reached. If the slot seal ruptured before this pressure was reached, the pressure at failure was recorded and the volume of effluent fluid was measured. If the seal held at 6.89 MPa, the pressure was maintained for 10 min before the test was terminated.

Test results from these slurries at an ambient temperature of 27° C are summarized in Table V. As indicated in the table, it appears that the sealing ability of fibreglass is directly related to the concentration of fibre added to the mud slurry. When the crack was only 1.5 mm wide, 1% fibrebridged slurry exhibited initial leakage at 0.14 MPa and finally failed under a pressure of 0.69 MPa. The pressure at failure was increased by a factor of ~ 7.0 by the addition of 3% fibre. Although this substantially increased the mud viscosity, a 5% increase in the concentration resulted in no filtrate losses at the required sealing pressure of

TABLE V Effect of fibreglass concentration on sealing ability

Fibreglass concentration (%)	Slot size (mm)	Sealing pressure (MPa)	Accumulated filtrate* (ml)
1	1.5	0	0
1	1.5	0.14	200
1	1.5	0.35	2750
1	1.5	0.69	3200
3	1.5	3.79	500
3	1.5	4.82	3000
5	1.5	6.89	0
5	4.0	0	0
5	4.0	0.14	2900
5	4.0	0.35	3200

*Maximum filtrate is 3500 ml.

6.89 MPa. However, when this mixture was used in conjunction with a 4.0 mm slot size, a large filtrate loss occurred at a pressure of only 0.14 MPa. Consequently, the fibre length of 6.25 mm appears to be insufficient to fully seal large-size fractures. These results suggest that further slot tests are necessary to evaluate longer fibres. In addition, the plugging activity of hydraulic cement in conjunction with the bridging materials should be studied at temperatures elevated up to 300° C.

4. Conclusions

Mixtures of hydraulic cement and water-based bentonite drilling fluids have a high potential for use in cementitious lost-circulation control materials in geothermal wells at temperatures up to 300° C. Prior to the current BNL work, when cement was added directly to bentonite fluids, the viscosity of the resultant slurry and its short thickening time at elevated temperatures made it very difficult to pump. In our current work, it was determined that the addition of a borax 10 mol ($Na_2B_4O_7 \cdot 10H_2O$) admixture to the bentonite fluid, before mixing with the cement, significantly acts to suppress the rate of complexations and bentonite hydrations and to retard the setting of the cement at elevated temperatures. The effectiveness of borax is due primarily to the Na^+ and $B_4O_7^{2-}$ ions dissociated by hydrolysis of borax in the bentonite fluids. The compensation Na^+ ions are strongly chemisorbed on the $Si–O^-$ located between the intersheets of montmorillonite. Once the negative silica sheets are neutrally balanced by Na^+ ions, the water-adsorbing capacity of the interlayers becomes very small. Thus, Na^+-saturated intersheets contribute to restrain the cement–bentonite complex coagulation and reduce the swelling of bentonite, thereby decreasing the viscosity of the mud slurries. After incorporation with cement, large numbers of $B_4O_7^{2-}$ counterions react rapidly with Ca^{2+} ions released from cement grains in colloidal bentonite–borax–cement–water phases. This nucleophilic attraction is associated with precipitation of a calcium-depleted silica gel and an impervious film of Ca^{2+}–$B_4O_7^{2-}$ complexation which covers the cement grain surfaces. These precipitations appear to provide an effective barrier which suppresses the propagation of cement hydrations. The great retarding activity of $B_4O_7^{2-}$ at temperatures up to 300° C was proved by the dramatic extension of the thickening time of the slurry following the addition of borax. It was also observed that the borax acts to expand the hardened CLCMs. A 7% borax-treated slurry exhibited a linear expansion of ~2.2%, as compared to the shrinkage characteristics of the control slurry after autoclaving.

In hardened bentonite–cement–borax–water systems, the major factor controlling both the compressive strength and water permeability was found to be the $CaO–SiO_2–H_2O$ (C–S–H) species formed under the hydrothermal conditions. The qualitative ranking of C–S–H groups affecting the properties of the autoclaved specimens in the temperature range of 200 to 300° C was estimated to be in order of tobermorite > xonotlite > scawtite and truscotite. The well-crystallized tobermorite responsible for the high-quality CLCM is essentially stable at a temperature around 200° C. Increasing the temperature to 300° C leads to the tobermorite–xonotlite and xonotlite–truscottite transformations.

Without the addition of a bridging additive material to the CLCM, a loss of a large amount of the slurry can be expected before the cement sets if large fractures are encountered in a lost-circulation zone. The use of a bridging material could effectively reduce flow through or seal off the fracture until the CLCM hardens. Chopped fibreglass was identified as an effective material for this use. Although the fibreglass used was susceptible to chemical disintegration in the hot alkaline solution, the C–S H crystal formation precipitated by a nucleophilic reaction between the silicate ions dissolved from the fibre surface and the Ca^{2+} ions from the cement under the hot alkaline conditions were shown to be effective as a protective layer to suppress further alkaline damage to the fibre, and as a crosslinking function which acts to improve the bond strength at the cement matrix–fibre interfaces. The ability of fibreglass to plug fractures of different sizes seems related to the concentration and the dimensions of the fibre added to the mud slurries.

Acknowledgements

The authors gratefully acknowledge Mr G. E. Loepke for performing the slot test and helpful discussions with Dr J. R. Kelsey and Mr B. C. Caskey, all of Sandia National Laboratories.

References

1. T. SUGAMA, L. E. KUKACKA, J. B. WARREN and B. G. GALEN *J. Mater. Sci.* **21** (1986) 2159.
2. J. U. MESSENGER, "Lost Circulation" (Penn Well, Tulsa, Oklahoma, 1981) p. 44.
3. G. POLK, W. R. CLEMENTS and G. SIMPSON, in Proceedings of Geothermal Well Drilling and Complation Workshop, Reno, May 1982.
4. J. U. MESSENGER, US patent 4 183 199 (1979).
5. *Idem*, US Patent 3 876 006 (1975).
6. D. D. DAMSON and W. C. GAINS Jr, *World Oil* (October 1953). 222.
7. M. A. GOODMAN, "Lost Circulation in Geothermal Wells: Survey and Evaluation of Industry Experience", SAND-81-7129 (1981).
8. Fann Instrument, Dresser Industries, Inc. (1983).
9. U. HOFFMAN, K. ENDELL and D. WILM, *Z. Krist.* **A86** (1933) 340.
10. C. E. MARSHALL, *ibid.* **A91** (1935) 433.

11. S. B. HENDRICKS, *J. Geol.* **50** (1942) 276.
12. Powder Diffraction File, Inorganic Phases, Card 12-219.
13. R. TURRIZIANI, A. RIO and M. COLLEPARDI, *Ind. Ital. Chem.* **35** (1965) 635.
14. J. F. YOUNG, H. S. TONG and R. L. BERGER, *J. Amer. Ceram. Soc.* **60** (1977) 193.
15. N. L. THOMAS and D. D. DOUBLE, *Cem. Concr. Res.* **11** (1981) 675.
16. K. LUKE and H. F. W. TAYLOR, *ibid.* **14** (1984) 657.
17. L. E. EILERS and R. L. ROOT, Paper SPE 5028 presented at SPE 49th Annual Fall Meeting, Houston, Texas, October 1974.
18. J. P. GALLUS and D. E. PYLE, Paper SPE 7591 presented at SPE 53rd Annual Fall Meeting, Dallas, Texas, October 1978.
19. G. L. KALOUSEK and E. B. NELSON, *Cem. Concr. Res.* **8** (1978) 283.
20. Owens-Corning Technical Information: "Textile Fibers For Industry" (1986).
21. T. E HINKEBEIN, V. L. BEHR and S. L. WILDE, "Static Slot Testing of Conventional Lost Circulation Materials", SAND-82-1080 (1983).

Received 15 January
and accepted 13 March 1986